

Supplement of

**A global surface CO₂ flux dataset (2015–2022) inferred from
OCO-2 retrievals using the GONGGA inversion system**

Text S1: Method for calculating prior and posterior uncertainties

For the flux optimization, the optimized variable is the scaling factor. The posterior flux is the product of the posterior scaling factor and the prior flux:

$$F_{t,i,j}^{post} = \lambda_{t,i,j}^{post} \times F_{t,i,j}^{prior}, \quad (S1)$$

where $F_{t,i,j}^{post}$ is the posterior carbon flux, $\lambda_{t,i,j}^{post}$ is the posterior scaling factor, and $F_{t,i,j}^{prior}$ is the prior carbon flux, t denotes the current t th window, i denotes the i th grid in longitude, and j denotes the j th grid in latitude. Both of fluxes and scaling factors are gridded variables with the same horizontal resolution as the transport model. To characterize the prior uncertainty of NEE and ocean carbon fluxes, the NLS-4DVar method applies an ensemble to approximate the prior error covariance matrix (Tian et al., 2018):

$$\mathbf{B}^{prior} = \frac{(\mathbf{P}_x^{prior})(\mathbf{P}_x^{prior})^T}{N-1}. \quad (S2)$$

where $\mathbf{P}_x^{prior} = (\mathbf{x}'_1, \mathbf{x}'_2, \dots, \mathbf{x}'_N)$ is an ensemble of prior perturbations, $\mathbf{x}'_j = \mathbf{x}_j - \mathbf{x}_a$, $j = 1, 2, \dots, N$, \mathbf{x}_j is the j th perturbation, and N is the number of prior perturbations. According to Evensen (2009), the ensemble of posterior perturbations after assimilation is calculated as follows:

$$\mathbf{P}_x^{post} = \mathbf{P}_x^{prior} \mathbf{V}_2 \sqrt{\mathbf{I} - \Sigma_2^T \Sigma_2} \Phi^T, \quad (S3)$$

where

$$\mathbf{U}_2 \Sigma_2 \mathbf{V}_2^T = \mathbf{X}_2, \quad (S4)$$

$$\mathbf{X}_2 = \Lambda^{-1/2} \mathbf{Z}^T \mathbf{P}_y, \quad (S5)$$

$$\mathbf{Z} \Lambda^{-1} \mathbf{Z}^T = [(\mathbf{P}_y)(\mathbf{P}_y)^T + (N-1)\mathbf{R}]^{-1}. \quad (S6)$$

and Φ is a random orthogonal matrix, $\mathbf{P}_y = h(\mathbf{P}_x^{prior}) - h(\mathbf{x}_a)$. Then, the prior (\mathbf{B}^{prior}) and posterior (\mathbf{B}^{post}) error covariance matrices can be calculated using \mathbf{P}_x^{prior} and \mathbf{P}_x^{post} , respectively, according to Eq. (S2). The prior perturbations of the scaling factor in the first inversion window were obtained through historical sampling, and prior perturbations in the following windows were generated through ensemble updating (Tian et al., 2020).

After obtaining the prior and posterior uncertainties of the scaling factors, the prior and posterior total flux uncertainties (σ_{total}^{prior} and σ_{total}^{post}) can be calculated according to the correlation between fluxes and scaling factors (Niwa and Fujii, 2020):

$$\sigma_{total}^{prior} = \sqrt{(\mathbf{F}^{prior})^T \mathbf{B}^{prior} (\mathbf{F}^{prior})}, \quad (S7)$$

$$\sigma_{total}^{post} = \sqrt{(\mathbf{F}^{prior})^T \mathbf{B}^{post} (\mathbf{F}^{prior})}. \quad (S8)$$

where we assume that the flux uncertainties are time independent.

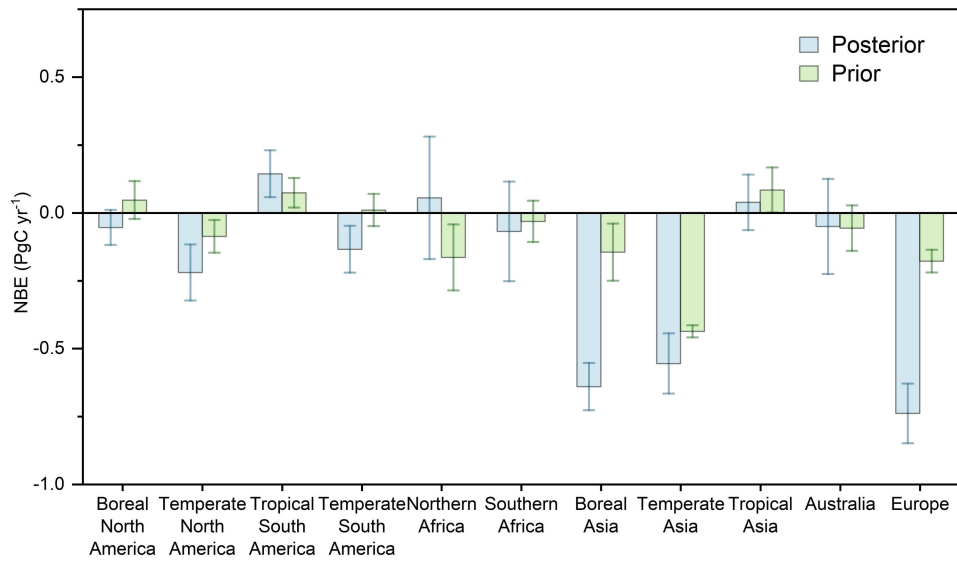


Figure S1. Annual mean (2015–2022) NBE at 11 TransCom land regions from GONGGA prior and posterior estimates. Error bar of NBE represents multi-year standard deviation.

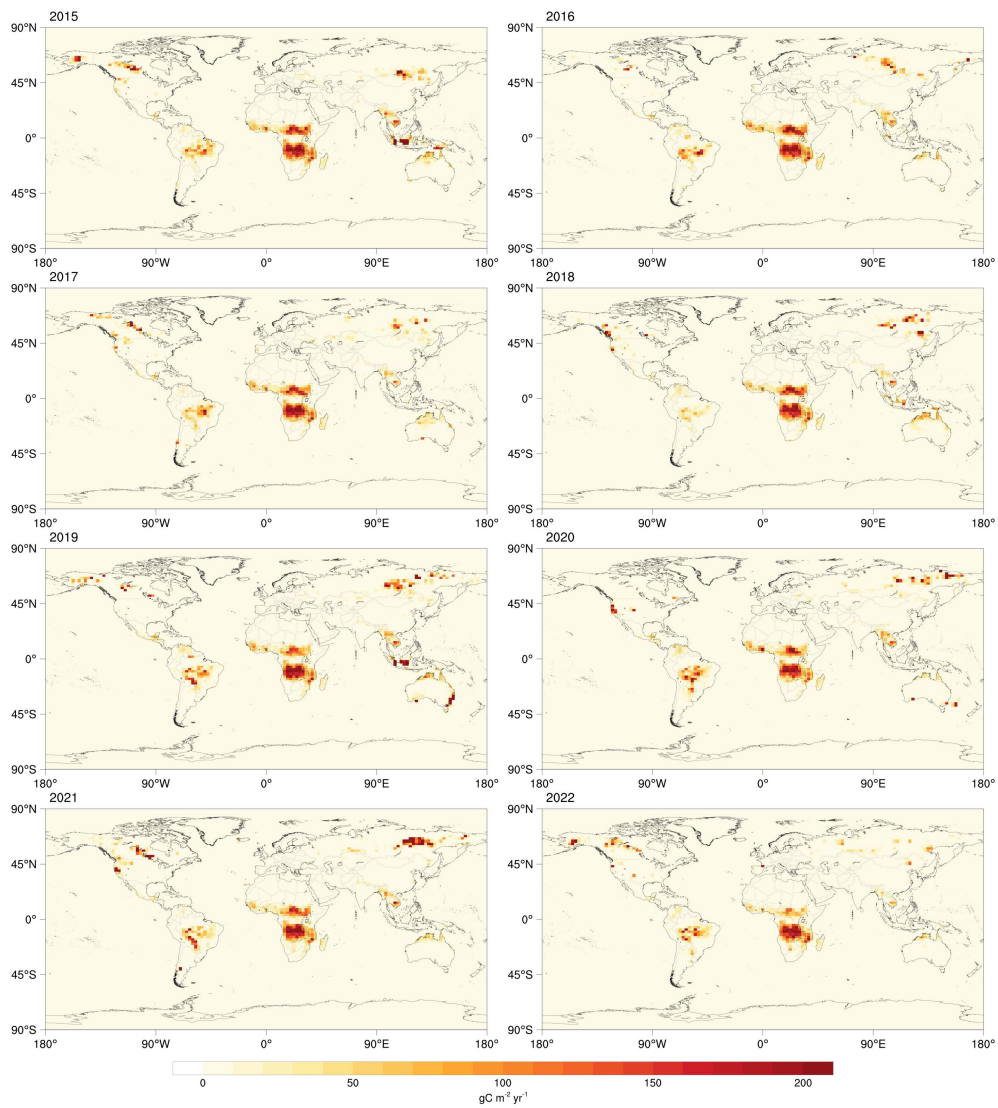


Figure S2. The spatial distribution of biomass burning emissions from GFED4.1s estimate during 2015–2022 period.

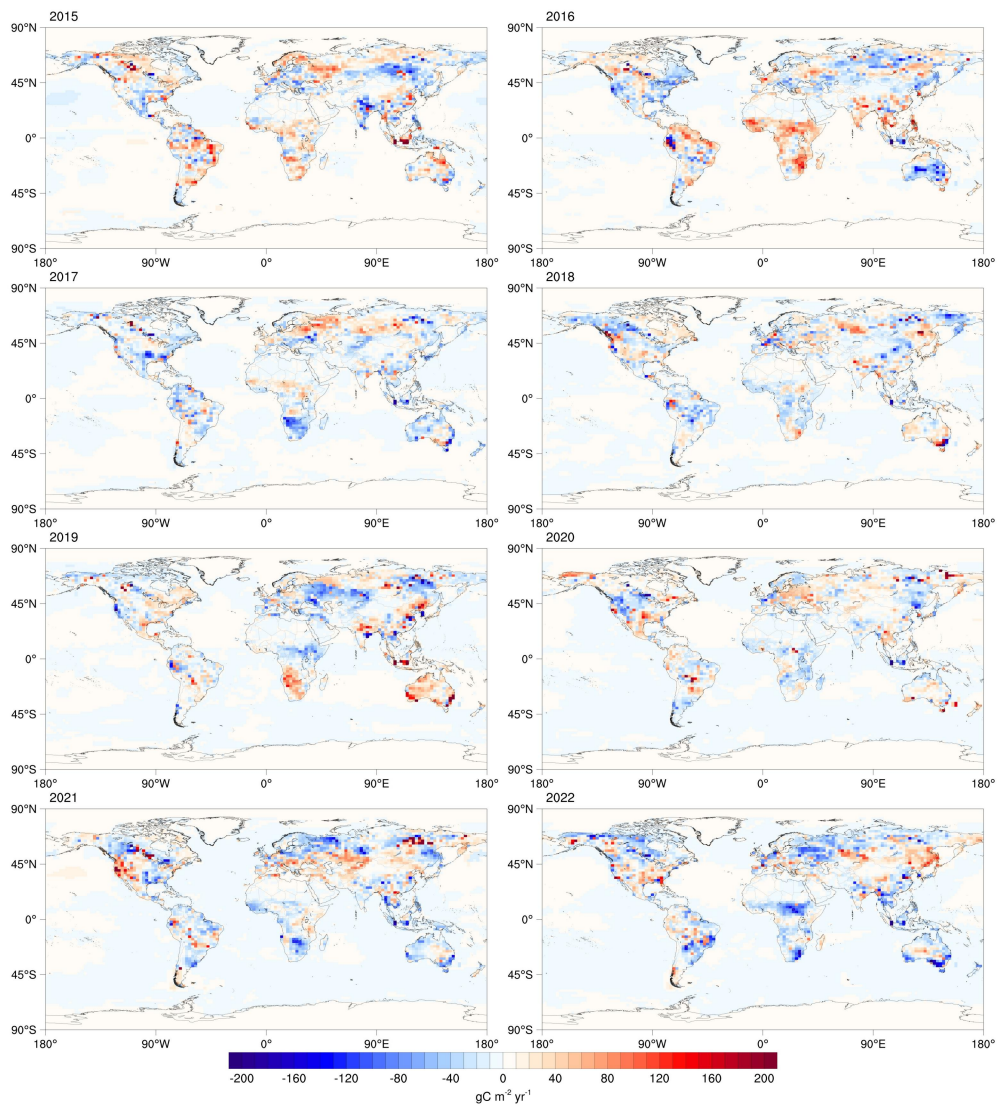


Figure S3. The annual NBE and ocean flux anomalies (annual value minus 8-year mean) during 2015–2022 period.

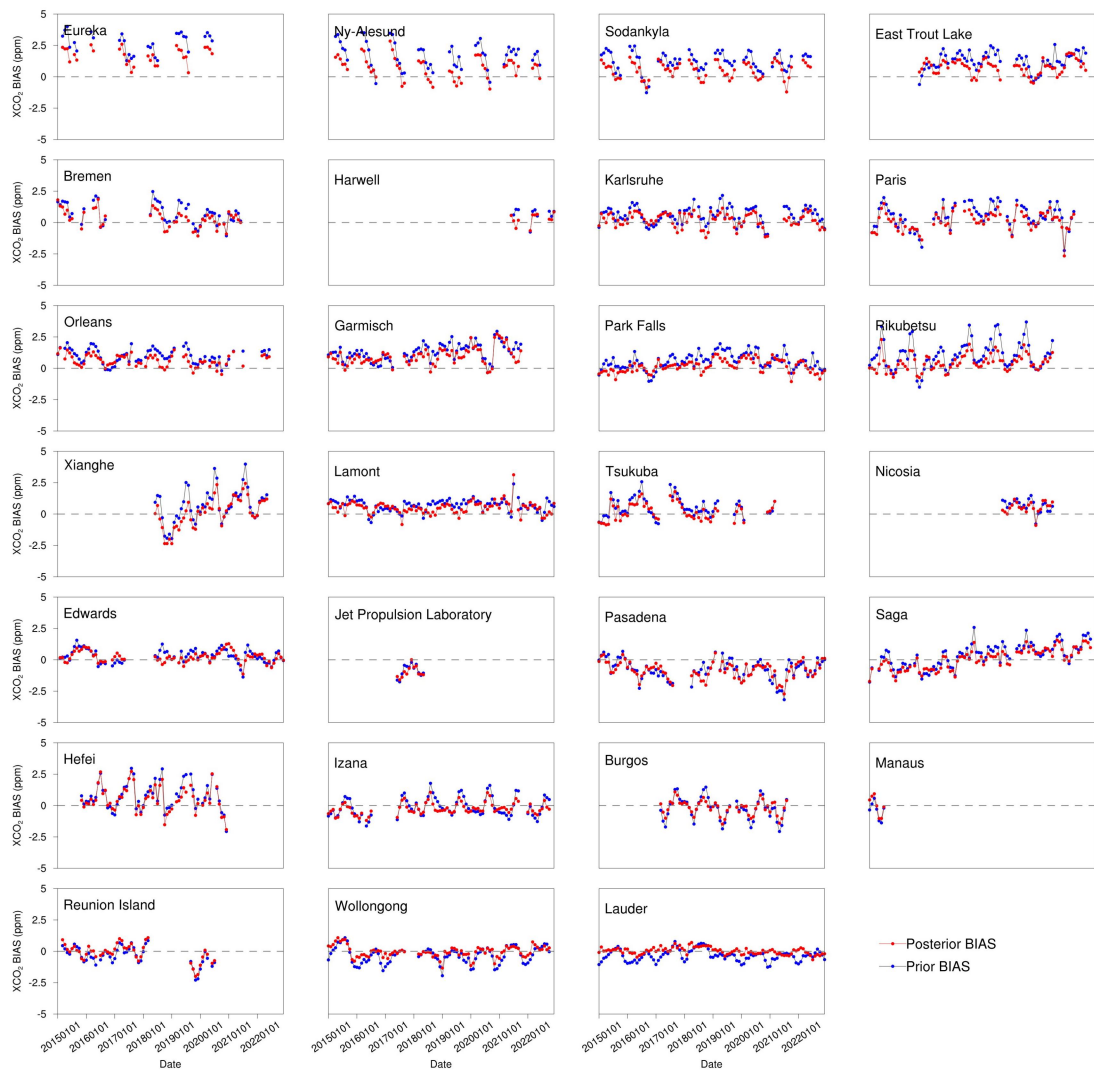


Figure S4. Time series of monthly averaged prior (blue) and posterior (red) simulated XCO₂ BIAS at each TCCON site (prior/posterior simulation – observation).

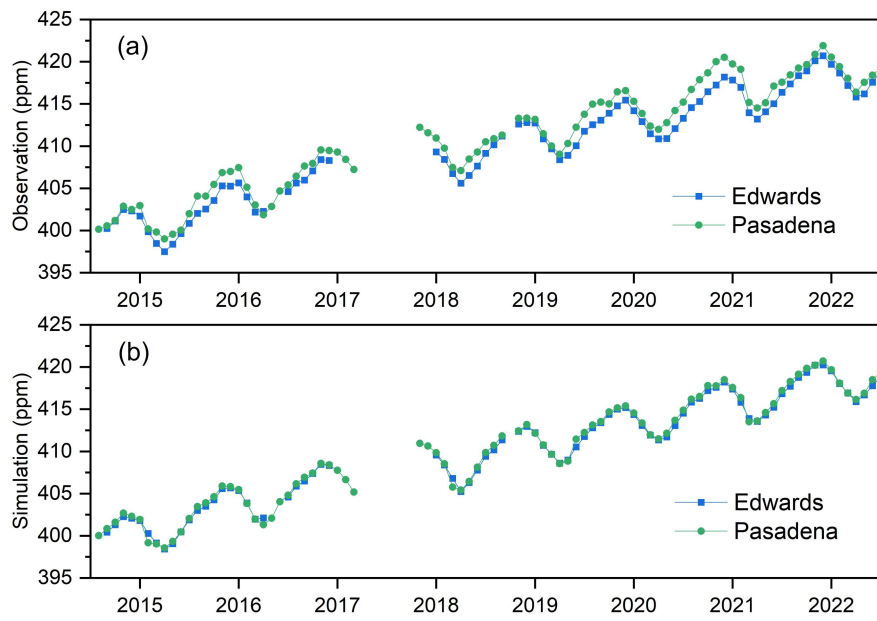


Figure S5. Time series of monthly (a) TCCON observations and (b) corresponding posterior simulations at Edwards (blue) and Pasadena (green) during 2015–2021 period.

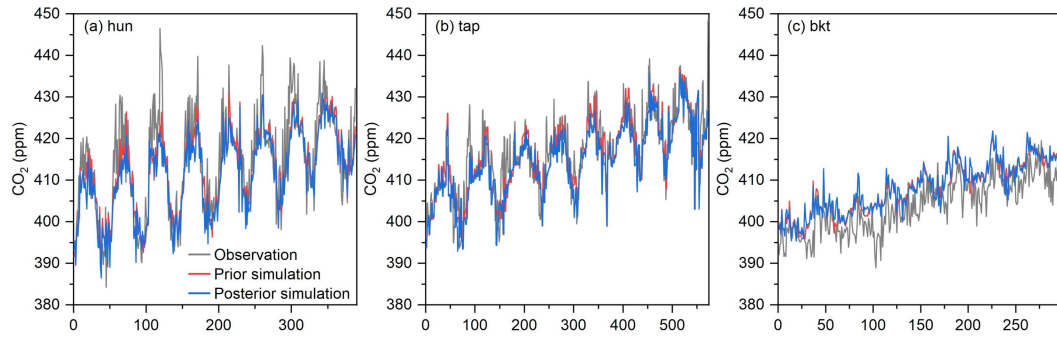


Figure S6. Time series of ObsPack surface flask observations as well as corresponding prior and posterior simulations at three sites that posterior RMSE exceed 4.0 ppm.

Table S1. OCO-2 MIP v10 participants and model details.

| Model | Contact | Institution | Transport Model | Meteorology | Inverse Method |
|-----------|---|--------------------------------------|-----------------|-------------|--------------------|
| Ames | Matthew Johnson and Sajeev Philip | NASA Ames Research Center | GEOS-Chem | MERRA-2 | 4D-Var |
| CAMS | Frédéric Chevallier | LSCE France | LMDz | ERA-interim | 4D-Var |
| COLA | Zhiqiang Liu | – | – | – | – |
| CMS-Flux | Junjie Liu | NASA JPL | GEOS-Chem | GEOS-FP | 4D-Var |
| CSU | Andrew Schuh | Colorado State University | GEOS-Chem | MERRA-2 | Bayesian synthesis |
| CT | Andy Jacobson | University of Colorado and NOAA GML | TM5 | ERA-interim | EnKF |
| JHU | Scot Miller | – | – | – | – |
| LoFI | Brad Weir | – | – | – | – |
| NIES | Shamil Maksyuotov | – | – | – | – |
| OU | Sean Crowell | University of Oklahoma | TM5 | ERA-interim | 4D-Var |
| PCTM | David Baker | Colorado State University | PCTM | MERRA-2 | 4D-Var |
| TM5-4DVAR | Sourish Basu | University of Maryland and NASA GMAO | TM5 | ERA-interim | 4D-Var |
| UT | Feng Deng | University of Toronto | GEOS-Chem | GEOS-FP | 4D-Var |
| WOMBAT | Michael Bertolacci, Andrew Zammit Mangion, Noel Cressie | University of Wollongong | GEOS-Chem | MERRA-2 | MCMC |

Table S2. Annual and six-year mean NBP at Boreal North America and Northern Africa from OCO-2 MIP v10 IS and LNLG experiments. Uncertainties are the one standard deviation spread in the inversion ensemble.

| Region | Year | Experiment | NBE (PgC yr ⁻¹) | Experiment | NBE |
|----------------------|------|------------|-----------------------------|------------|--------------|
| Boreal North America | 2015 | IS | -0.28 ± 0.36 | LNLG | -0.22 ± 0.56 |
| | 2016 | | -0.36 ± 0.37 | | -0.11 ± 0.49 |
| | 2017 | | -0.34 ± 0.38 | | -0.22 ± 0.53 |
| | 2018 | | -0.40 ± 0.33 | | -0.21 ± 0.53 |
| | 2019 | | -0.46 ± 0.37 | | -0.27 ± 0.59 |
| | 2020 | | -0.44 ± 0.48 | | -0.07 ± 0.53 |
| | Mean | | -0.38 ± 0.38 | | -0.18 ± 0.54 |
| Northern Africa | 2015 | IS | 0.23 ± 1.42 | LNLG | 0.87 ± 0.89 |
| | 2016 | | 0.65 ± 1.42 | | 1.24 ± 0.88 |
| | 2017 | | 0.32 ± 1.40 | | 0.90 ± 0.95 |
| | 2018 | | 0.01 ± 1.26 | | 0.70 ± 0.87 |
| | 2019 | | 0.24 ± 1.15 | | 0.73 ± 0.85 |
| | 2020 | | 0.34 ± 1.18 | | 0.64 ± 0.92 |
| | Mean | | 0.30 ± 1.31 | | 0.85 ± 0.90 |

Reference

- Evensen G, 2009. Data assimilation: The ensemble kalman filter. Springer-Verlag Berlin Heidelberg, 307 pp.
- Niwa Y, Fujii Y. 2020. A conjugate bfgs method for accurate estimation of a posterior error covariance matrix in a linear inverse problem. Quarterly Journal of the Royal Meteorological Society, 146(732): 3118-3143
- Tian X, Han R, Zhang H. 2020. An adjoint-free alternating direction method for four-dimensional variational data assimilation with multiple parameter tikhonov regularization. Earth and Space Science, 7(11)
- Tian X, Zhang H, Feng X, Xie Y. 2018. Nonlinear least squares en4dvar to 4denvar methods for data assimilation: Formulation, analysis, and preliminary evaluation. Monthly Weather Review, 146(1): 77-93